Molecular Biology of the Cell
Vol. 19, 2241–2250, May 2008

The Mood Stabilizer Valproate Inhibits both Inositol- and Diacylglycerol-signaling Pathways in *Caenorhabditis elegans*

Suzumi M. Tokuoka,*† Adolfo Saiardi,‡ and Stephen J. Nurrish†

MRC Cell Biology Unit, MRC Laboratory for Molecular Cell Biology, †Departments of Neuroscience, Physiology, and Pharmacology and ‡Cell and Developmental Biology, University College London, London WC1E 6BT, United Kingdom

Submitted September 28, 2007; Revised February 5, 2008; Accepted February 13, 2008
Monitoring Editor: Thomas F. J. Martin

The antiepileptic valproate (VPA) is widely used in the treatment of bipolar disorder, although the mechanism of its action in the disorder is unclear. We show here that VPA inhibits both inositol phosphate and diacylglycerol (DAG) signaling in *Caenorhabditis elegans*. VPA disrupts two behaviors regulated by the inositol-1,4,5-trisphosphate (IP_3): defecation and ovulation. VPA also inhibits two activities regulated by DAG signaling: acetylcholine release and egg laying. The effects of VPA on DAG signaling are relieved by phorbol ester, a DAG analogue, suggesting that VPA acts to inhibit DAG production. VPA reduces levels of DAG and inositol-1-phosphate, but phosphatidylinositol-4,5-bisphosphate (PIP_2) is slightly increased, suggesting that phospholipase C-mediated hydrolysis of PIP_2 to form DAG and IP_3 is defective in the presence of VPA.

INTRODUCTION

Bipolar disorder is a prevalent and devastating illness, which is characterized by mood swings between depression and mania. VPA reduces mood swings in bipolar patients, although its mechanism of action is controversial (Harwood, 2005). Several lines of evidence suggest that VPA interferes with inositol phosphate signaling. For example, it decreases myoinositol levels in the mouse and rat brain (O'Donnell *et al*., 2000; Shaltiel *et al*., 2004) and inositol-1,4,5-trisphosphate [Ins(1,4,5)P_3, henceforth referred to as IP_3] in *Dictyostelium* (Williams *et al*., 2002). Moreover, another bipolar treatment, lithium (Li^+), is known to alter inositol signaling by inhibition of two enzymes critical for inositol recycling: inositol-1(or 4)-monophosphatase (IMPase) (Allison *et al*., 1980; Hallcher and Sherman, 1980) and inositol-1,4-bisphosphate 1-phosphatase (IPPase) (Inhorn and Majerus, 1987). Thus, it has been suggested that bipolar disorder is associated with defective neuronal inositol phosphate signaling, which can be alleviated by drugs that modulate these signaling pathways.

Inositol is essential for the production of phosphatidylinositol-4,5-bisphosphate [PI(4,5)$_2$P, henceforth referred to as PIP_2], which is a signaling molecule in its own right. PIP_2 can give rise to many other molecules that alter neuronal activity. For example, PIP_2 can be hydrolyzed by phospholipase C (PLC) to DAG and IP_3; DAG activates neuroregulators such as UNC-13 and protein kinase C (PKC), IP_3 binds to the IP_3 receptor (IP_3R), triggering the release of Ca^{2+} from the ER. Both DAG and Ca^{2+} are important regulators of synaptic efficacy and plasticity. IP_3 can be both phosphorylated and dephosphorylated on multiple positions to give rise to other inositol phosphates, some of which have been implicated in the control of vesicle fusion and recycling (De Camilli *et al*., 1996; McPherson *et al*., 1996; Fukuda and Mikoshiba, 1997; Acharya *et al*., 1998). PIP_2 can also be phosphorylated to PIP_3, which has been implicated in control of synaptic plasticity and learning and memory (Raymond *et al*., 2002; Horwood *et al*., 2006; Karpova *et al*., 2006). Thus, changes in inositol signaling by drugs such as VPA would be expected to alter neuronal function. However, the role of inositol signaling in bipolar disorder and its treatment remain controversial. VPA has other targets that are unrelated to inositol signaling; it potentiates GABAergic neurotransmission (Loscher, 1999), for example, and it inhibits histone deacetylase transcriptional repressors. Thus, VPA could potentially alter levels of transcription via multiple routes (Phiel *et al*., 2001).

To better understand VPA action, we have taken advantage of *Caenorhabditis elegans* as a genetic model system. *C. elegans* has a simple nervous system, but it possesses many of the components involved in mammalian synaptic transmission. By combining behavioral assays and genetics, we describe for the first time that VPA alters *C. elegans* behaviors in two ways. First, VPA alters inositol phosphate-regulated behaviors in *C. elegans*. Second, we show that VPA inhibits DAG-regulated behaviors most likely by inhibiting DAG signaling via UNC-13. This is the first report of an effect of VPA on DAG signaling.

MATERIALS AND METHODS

Strains

All strains were cultivated at 20°C, and they were maintained as described previously (Brenner, 1974). The wild-type N2, *egl-8(md1971)*, *pkc-1(nj3)* (Oko-

This article was published online ahead of print in *MBC in Press* (http://www.molbiolcell.org/cgi/doi/10.1091/mbc.E07–09–0982) on February 20, 2008.

* Present address: Department of Biochemistry and Molecular Biology, Faculty of Medicine, The University of Tokyo, 7-3-1 Hongo, Bunkyo-ku, Tokyo 113-0033, Japan.

Address correspondence to: Stephen J. Nurrish (s.nurrish@ucl.ac.uk).

chi *et al*., 2005), *itr-1(sy327)unc-24(e138)*, and *unc-24(e138)* strains were obtained from the *Caenorhabditis* Genetics Center (University of Minnesota, Minneapolis, MN). The gain-of-function *itr-1(sy327)* mutation is only available marked with the closely linked *unc-24(e138)* mutation as *itr-1(sy327)* has no obvious visible phenotype. We have been unable to obtain recombinants carrying only the *itr-1(sy327)* mutation. Other strains have been described previously: *egl-8(md1971)* (Lackner *et al*., 1999; Miller *et al*., 1999) and *unc-13(s69);nuIs46(UNC-13(+)*(Sieburth *et al*., 2006). QT181 *unc-13(s69)*; *nzIs25* expresses *UNC-13*(H173K)::GFP in a putative null *unc-13(s69)* background (McMullan *et al*., 2006). KP1683 *nuIs59* expresses *rol-6(gf)*, *UNC-13*::YFP and p.acr-2::CFP::SNB-1 (Nurrish *et al*., 1999). The strain expressing *p.rab-3::PHPLC-∂1::GFP* as an extrachromosomal array also containing the *rol-6* marker was a gift from G. Lesa (MRC Laboratory for Molecular Cell Biology, London, United Kingdom), and it is described in Marza *et al*. (2007).

Preparation of Assay Plates

Assay plates for all the experiments were made 1 day before the assays. NaCl-, VPA-, or LiCl-containing plates were made by adding the drug stock solutions (dissolved in water) to melted nematode growth medium (NGM) agar with standard supplements (Brenner, 1974). Standard food stocks were made by growing OP50 in Luria Broth (OD_{600} of 0.2–0.3) and then centrifuging the bacteria to make a 100-fold concentrated bacterial suspension. Suspension (100 μl) was seeded to each drug-containing NGM agar plate of 55 mm in diameter. The suspension usually spread to ~30 mm in diameter. Seeded plates were allowed to dry for 1–2 h before use in assays.

Defecation Assay

First-day adult animals (22–24 h after larval [L]4 stage) were transferred onto drug-containing seeded plates, and then the posterior body contraction (pBoc) and enteric muscle contractions (EMCs) were recorded using the Etho program (obtained from Jim Thomas, University of Washington, Seattle, WA) between 60 and 120 min after the transfer. For each drug concentration, a minimum of eight different animals were scored for 5 min from the first posterior body contraction. If the animal moved off from bacterial lawn during the observation, it was not recorded.

Analysis of Brood Size, Sheath Contraction, and Ovulation

Adult animals (2 d after L4 stage) were placed on 6 mM NaCl- or 6 mM VPA-containing plate for 3.5 h, and then they were anesthetized in M9 solution containing 0.1% tricaine, 0.01% tetramisole, and 6 mM NaCl or 6 mM VPA for 20 min. Ovulation and sheath cell contraction were observed as described previously (McCarter *et al*., 1999; Yin *et al*., 2004). Brood size was quantified by transferring L4s to fresh drug-containing plates every day for 5 d. The number of F1 progeny on each plate was counted 1 d after eggs hatched.

Growth Assay

Eight to 12 young adult animals (24–26 h post-L4 stage) were placed on drug-containing plate, and then they were allowed to lay eggs for ~1 h until 50–60 eggs were laid. The adults were removed, and eggs were left to hatch and develop at 20°C. After 3 and 4 d, the percentage of adult animals on the plates was counted, and representative pictures were taken.

Aldicarb and Levamisole Assays

First-day adult animals (22–24 h after L4 stage) were first placed on plates containing 12 mM NaCl or 12 mM VPA, and, where indicated, 0.25 μg/ml phorbol 12-myristate 13-acetate (PMA) (Sigma Chemical, Poole, Dorset, United Kingdom) or 25 μg/ml methiothepin (Sigma Chemical) for 2 h. Animals were then placed on the same plates, except they also contained either 1 mM aldicarb or 100 μM levamisole. Onset of paralysis was measured as described previously (Nurrish *et al*., 1999). These assays were performed blind with respect to drug treatments and strains. For each experiment, 25–30 animals were tested, and each experiment was repeated at least four times.

Microscopy

Animals expressing UNC13S::YFP; *p.acr-2*::SNB-1::CFP (*nzIs59*) were imaged by mounting on agarose pads, and they were viewed using a Leica TCS SPE confocal microscope with a Leica 63× ACS APO, with a numerical aperture of 1.3. Images were obtained using Leica LAS AF software. Images were blinded with respect to treatment and the eight-bit images were analyzed using ImageJ (http://rsb.info.nih.gov/ij/). *UNC-13*::YFP and SNB-1::CFP puncta numbers per 10 μm were counted as described previously (McMullan *et al*., 2006). PHPLC-∂1::GFP punctual and interpuncta fluorescent values were obtained as described in Marza *et al*. (2007). Essentially, the images were thresholded, and a puncta was defined as any object within the neuronal process compose of more than five pixels with a value >150 (fluorescent values of an 8-bit image range from 0 to 255). The interpunctal regions were the parts of the neuronal process with a value <150. Eleven wild-type animals exposed to 12 mM NaCl and 11 animals exposed to 12 mM VPA were imaged. Quantification was performed blind to drug treatment.

Egg-laying Assay

Eight young adults (24–26 h after the L4 stage) were placed on a 6 mM NaCl- or 6 mM VPA-containing assay plate, and they were allowed to lay eggs for 2 h. The adults were removed, and the remaining eggs (referred to as "on plate") were counted. The adults were individually dissolved with alkaline bleach solution on unseeded agar plates, and their eggs, which were not dissolved because of their protective eggshells, were counted (referred to as "in worm"). For each condition, five independent experiments were carried out. For PMA experiments, assay plates containing 2 μg/ml phorbol ester (Sigma Chemical) were used.

RNA Interference (RNAi) of Myoinositol-1-phosphate Synthase (MIP Synthase; VF13D12L.1)

RNAi gene knockdown was induced by feeding worms with *Escherichia coli* (strain HT115) producing double-stranded RNA (dsRNA). Bacteria containing the L4440 vector with inserts of the *C. elegans* MIP synthase (VF13D12L.1) (Kamath *et al*., 2003) were obtained from MRC Geneservice. NGM plates containing 25 μg/ml carbenicillin and 1 mM isopropyl β-D-thiogalactoside were allowed to dry overnight before seeding. Bacteria were cultured for 24 h at 37°C in L-Broth containing 50 μg/ml ampicillin, and then they were seeded onto plates. The next day, 4–6 L1 stage larvae were synchronized by treating first-day adults with alkaline bleach on unseeded plates the day before, and they were transferred onto feeding plates and left to develop at 20°C. For defection assay, L4 progenies were transferred to new feeding plates seeded with the bacteria, and defecation assays were performed after 22–24 h. For growth assay, the resultant adults were transferred to new plates seeded with the bacteria, and they were allowed to lay eggs for ~1 h until the number of eggs reached 50–60. Adults were removed, and eggs were left to hatch and develop at 20°C. HT115 bacteria transformed with the L4440 vector without an insert were used as an RNAi control.

Quantification of Inositol Phosphates

Three L4s were placed on NGM agar plates seeded with *Escherichia coli* strain OP50, and after 4 d animals were washed off the plates to start a liquid culture. Two 55-mm plates were used for each 10-ml culture. Harvested animals were grown in S medium (Stiernagle, 2006) supplemented with 200 μg/ml streptomycin, 10 μg/ml nystatin, and 10 μCi/ml *myo*-[1,2-^{3}H]inositol (American Radiolabeled Chemicals, St. Louis, MO) at 20°C for 4 d. Every day, concentrated *E. coli* (strain HB101) was supplemented as food. Twenty-four hours before the end of the culture, NaCl, VPA, or LiCl was added to the culture at the final concentration of 12 mM. The measurement of radioactive inositol phosphates was performed as described previously (Azevedo and Saiardi, 2006), with some modification. Briefly, animals were collected and centrifuged, and washed three times with cold distilled water. Worms were first frozen on dry ice, and then an equal volume of 1 M ice-cold $HClO_4$ containing 3 mM EDTA was added, followed by vortexing for 10 min with an equal volume of glass beads (423–600 μm; Sigma Chemical). The samples were neutralized by an equal volume of 1 M K_2CO_3 containing 3 mM EDTA, and then they were centrifuged to remove precipitates before high-performance liquid chromatography (HPLC) analysis. The composition of inositol phosphates was assessed using a 4.6- × 125-mm Partisphere SAX column (Whatman, Maidstone, United Kingdom). The column was eluted with a gradient generated by mixing buffer A (1 mM EDTA) and buffer B [buffer A plus 1.3 M $(NH_4)_2HPO_4$, pH 3.8, with H_3PO_4] as follows: 0–5 min, 0% B; 5–10 min, 0–20% B; 10–70 min, 20–100% B; and 70–80 min, 100% B. The fractions (1 ml) were collected and counted using 4 ml of Ultima-Flo AP LCS-mixture (PerkinElmer Life and Analytical Sciences, Boston, MA). The ratio of inositol 1,3,4,5,6 pentakisphosphate and hexakisphosphate (IP_6) to inositol monophosphate (IP_1) was smaller than those observed from mammalian cells (observation by A.S.). This could reflect insufficient labeling time or a genuine different in inositol phosphate levels between *C. elegans* and mammals.

Statistics

Unpaired Student's *t* test (two-tailed) or multiple comparisons with Scheffé post hoc tests were used as required for all experiments except for the defecation assay. Because some defecation data were highly variable and did not show a normal distribution, we used nonparametric tests. For comparison of two groups, the Mann–Whitney test was used. For comparison of more than three groups, the Kruskal–Wallis test was first performed, and then when it was significantly different, the Mann–Whitney test was performed to compare each pair of groups. Data are shown as mean ± SEM.

RESULTS

VPA Disrupts Defecation, a Known IP_3-mediated Behavior

To investigate the action of VPA on inositol phosphate signaling in *C. elegans*, we compared the effects of VPA with

Li^+, a known inhibitor of enzymes required for inositol phosphate recycling. We began by testing the effects of VPA and Li^+ on defecation, which is known to be regulated by IP_3. The *C. elegans* defecation cycle is characterized by the contraction of three distinct sets of muscles every 50 s (Thomas, 1990). It begins with contraction of the posterior body wall muscles (pBoc), which is then followed by the relaxation of these muscles and the contraction of the anterior body wall muscles; finally, the enteric muscles contract, resulting in expulsion of the gut contents. Either mutations in IP_3R (*itr-1*) or overexpression of the IP_3 binding domain of the receptor from a ubiquitous heat-shock promoter causes a large increase in the time between defecation cycles (Dal Santo *et al*., 1999; Walker *et al*., 2002). VPA (valproic acid sodium salt) increased the mean defecation cycle length (defined as the time between pBoc steps) in a dose-dependent manner; LiCl also increased mean defecation cycle length, although to a lesser extent, whereas NaCl had no effect (Figure 1A). In addition, VPA increased the variability of defecation cycle length, as shown by defecation cycles for representative animals in Figure 1B. We quantified this by determining the coefficient of variance of defecation cycle length (Figure 1C). LiCl also increased the variability of defecation cycle length, to a lesser extent (Figure 1, B and C).

We confirmed that changes in inositol phosphate signaling caused the defecation defects by using RNAi to inhibit MIP synthase (VF13D12L.1), which catalyzes the conversion of glucose-6-phosphate to inositol-1-phosphate, the rate-limiting step in de novo inositol synthesis. The inhibition of MIP synthase increased defecation cycle length, consistent with a role for inositol and its derivatives in control of defecation cycle length (Figure 1D). RNAi knockdown of MIP synthase slightly increased the variability of defecation cycle length (Figure 1, E and F); however, this was not statistically significant. This may be due to incomplete RNAi knockdown of MIP synthase in all animals, alternatively MIP synthase and the target of VPA may act at different points in the inositol phosphate-signaling pathway. Nonetheless, the similarity between VPA, Li^+ and RNAi knockdown of MIP synthase on defecation behavior suggests that VPA affects inositol phosphate signaling. We also found VPA, Li^+, and RNAi knockdown of MIP synthase caused slow growth (Supplemental Figure 1). Slow growth is also caused by mutations in the IP_3 receptor ITR-1 (Dal Santo *et al*., 1999). Again, this is consistent with a model in which VPA inhibits inositol phosphate signaling.

VPA Inhibits Ovulation

In *C. elegans*, ovulation occurs when an oocyte triggers contractions in the surrounding sheath cells, eventually resulting in the oocyte entering into the spermatheca where it is then is fertilized. IP_3 receptor mutations decrease both contractions of the sheath cells surrounding the oocyte and ovulation itself (Clandinin *et al*., 1998; Miller *et al*., 2003; Yin *et al*., 2004). Mutations that decrease IP_3 synthesis also decrease both ovulation and sheath cell contractions; these include RNAi knockdowns of the phosphatidylinositol-4-phosphate 5′ kinase (*ppk-1*) and the PLCγ (PLC-3) (Yin *et al*., 2004; Xu *et al*., 2007). Defects in ovulation lead to a decreased brood size and addition of VPA strongly decreased brood size (Figure 2A). Exposure to VPA for 4 h also decreased ovulation (1.7 ± 0.2 per hour in the presence of NaCl compared with 0.7 ± 0.2 per hour in the presence of VPA) (Figure 2B). VPA also decreased the basal sheath cell contraction rate (9.0 ± 0.6 contractions per minute on NaCl compared with 5.3 ± 0.6 contractions per minute in the presence of VPA) (Figure 2C). These results are consistent with a model in which VPA decreases IP_3 signaling.

An IP_3 Receptor Gain of Function Mutation Suppresses the Effect of VPA on Defecation and Basal Sheath Cell Contraction Rate

Defects in IP_3 production can be suppressed by gain of function mutations in the IP_3 receptor *itr-1(sy327)*. Phospholipase Cγ PLC-3 produces IP_3 in response to LET-23 tyrosine kinase receptor activation. RNAi knockdown of PLC-3 causes defecation defects, an increase in the mean and coefficient of variance of defecation cycle time, and ovulation defects. Both the defecation and ovulation defects of RNAi knockdown of PLC-3 are suppressed by the *itr-1(sy327)* gain-of-function mutation (Yin *et al*., 2004; Espelt *et al*., 2005), which supports a role for ITR-1 downstream of PLC-3 and IP_3 production. We obtained animals in which the *itr-1(sy327)* mutation was linked to *unc-24(e138)* (0.14 cM apart), and we have been unable to isolate *itr-1(sy327)* single mutants. Therefore, we compared the effect of VPA between *itr-1(sy327)* unc-24*(e138)* double mutants and *unc-24(e138)* single mutants. Single *unc-24*(*e138*) mutants had a slightly

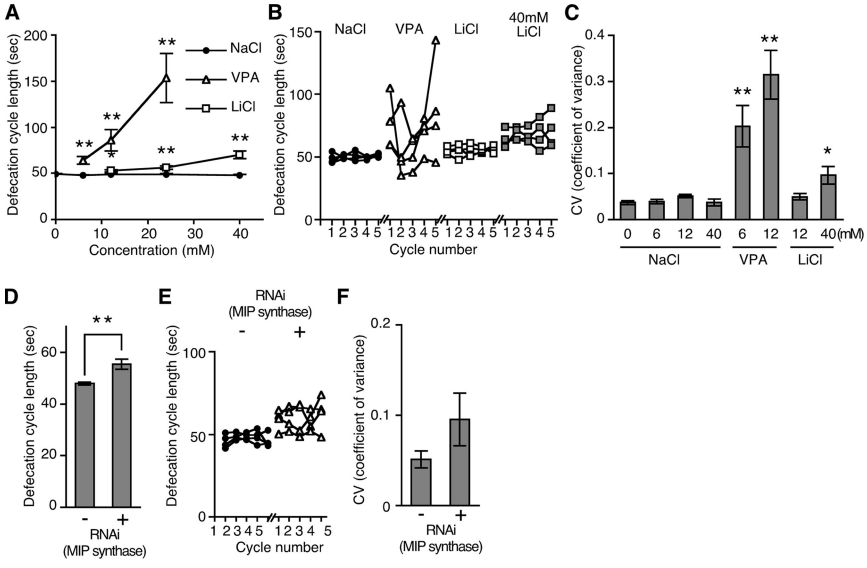

Figure 1. VPA affects defecation behaviors. (A) Exposure to VPA and Li^+ increased *C. elegans* defecation cycle length in a dose-dependent manner. (B) Examples of defecation cycle length variability of individual animals exposed to 12 mM NaCl, 12 mM VPA, 12 mM LiCl, or 40 mM LiCl. VPA, but not Li^+, greatly increased the variability of cycle length from one cycle to the next. (C) The coefficient of variance (SD divided by the mean) of defecation cycle length of animals exposed to the indicated drug concentrations. VPA causes defecation cycle length to become irregular. (D) RNAi knockdown of MIP synthase caused an increase in average defecation cycle length. (E) Examples of defecation cycle length of four individual animals from D are shown. (F) RNAi knockdown of MIP synthase increased the variability of defecation cycle length. However, the effect was not statistically significant ($p > 0.06$). Except B and E each data point represents mean ± SEM from eight to 22 animals. *$p < 0.05$ and **$p < 0.01$; Mann–Whitney test, compared with NaCl controls at the same concentration.

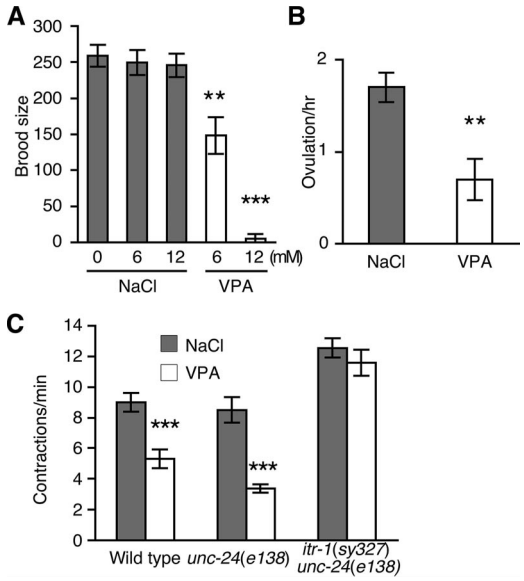

Figure 2. VPA reduces brood size, ovulation, and gonadal-sheath cell contractions. (A) VPA reduced the brood size of wild-type animals. (B) VPA (6 mM) reduced ovulation (passage of an oocyte into the spermatheca). (C) VPA (6 mM) reduced the basal sheath cell contraction rate in wild-type and control *unc-24(e138)* animals, but not in animals possessing an *itr-1* gain-of-function mutation [*itr-1(sy327) unc-24(e138)*]. **$p < 0.01$ and ***$p < 0.001$; Student's test, compared with NaCl controls at the same concentration. Each data point represents mean ± SEM from 10 animals.

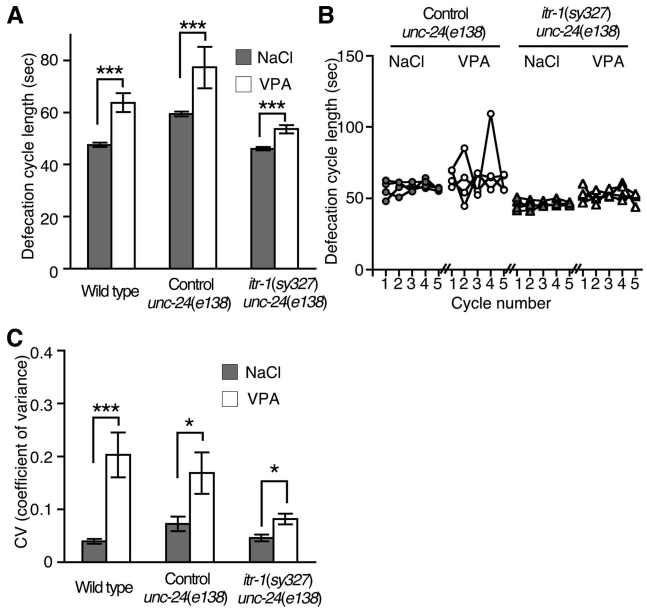

Figure 3. An IP_3 receptor gain-of-function mutation suppresses the effects of VPA. (A) Exposure to 6 mM VPA increased the mean defecation cycle length of *itr-1(sy327)* unc-24*(e138)* animals less than wild-type or control *unc-24(e138)* animals. (B) Examples of defecation cycle length variability of individual animals exposed to 6 mM NaCl or 6 mM VPA. (C) Coefficient of variance of animals exposed to 6 mM NaCl or 6 mM VPA. VPA increased the variability of defecation cycle length less in *itr-1(sy327)* unc-24*(e138)* animals compared with wild-type or control *unc-24(e138)* animals. In A and C, each data point represents mean ± SEM from 10 to 17 animals. *$p < 0.05$ and ***$p < 0.001$; Mann–Whitney test.

elongated defecation cycle, however, the cycle was elongated in response to VPA addition equivalent to that of wild-type animals (Figure 3A). The ability of VPA to increase defecation cycle length was strongly reduced by the *itr-1(sy327)* gain-of-function mutation [VPA-mediated increases in mean defecation cycle length were 16.3 ± 4.0 s in wild type, 15.0 ± 7.8 s in *unc-24(e138)*, and 7.4 ± 1.6 s in *itr-1(sy327)* unc-24*(e138)* double mutants]. VPA-mediated increases in the variability of defecation cycle length were also strongly suppressed by the *itr-1(sy327)* gain-of-function mutation (Figure 3, B and C). We also tested whether the *itr-1(sy327)* gain-of-function mutation also suppressed VPA defects in the IP_3-regulated basal sheath cell contractions. VPA decreased the sheath cell contraction rate of *unc-24(e138)* control animals; however, *itr-1(sy327)* unc-24*(e138)* double mutants were not affected by VPA (Figure 2C). These results demonstrate that VPA disrupts signaling upstream of the IP_3 receptor to cause defective defecation and ovulation.

VPA Inhibits DAG-stimulated Acetylcholine (ACh) Release

Hydrolysis of PIP_2 produces both IP_3 and the membrane-bound second messenger DAG. DAG regulates neurotransmitter release in both *C. elegans* and mammalian neurons (Betz *et al*., 1998; McMullan and Nurrish, 2007). Mutations in genes required for DAG signaling, including genes that encode the PLCβ EGL-8 (Lackner *et al*., 1999; Miller *et al*., 1999) and the DAG-binding neuroregulator UNC-13 (Lackner *et al*., 1999; Nurrish *et al*., 1999; Richmond *et al*., 1999), reduce ACh release. We determined the effect of VPA on ACh release using the acetylcholinesterase inhibitor aldicarb. Aldicarb prevents the removal of endogenously released ACh, resulting in a build up of ACh to a level sufficient to hypercontract the body wall muscles; this causes paralysis in wild-type animals but not in mutants that are defective in ACh release (Nonet *et al*., 1993; Nguyen *et al*., 1995; Miller *et al*., 1996). Animals exposed to VPA became paralyzed more slowly compared with untreated animals or animals exposed to NaCl, suggesting that VPA decreases levels of ACh release (Figure 4A). To determine whether VPA acted pre- or postsynaptically, we also measured rates of paralysis to the nicotinic agonist levamisole. Levamisole causes muscle hypercontraction and paralysis at a rate dependent on muscle sensitivity to ACh. VPA exposure resulted in an increased rate of paralysis compared with NaCl (Supplemental Figure 2A). Thus, when exposed to VPA, animals became paralyzed more slowly in response to aldicarb even though their muscles became more sensitive to ACh, suggesting that VPA decreased ACh release more strongly than suggested by the aldicarb assay. To test whether VPA inhibits ACh release via changes in DAG signaling, we tested the response to VPA in animals either defective for DAG production or defective for DAG signaling. Mutations in the *egl-8* PLCβ decrease levels of DAG production and result in lowered levels of ACh release (Lackner *et al*., 1999; Miller *et al*., 1999). DAG acts to increase ACh release in part through the recruitment of the DAG-binding neuromodulator UNC-13 to sites of neurotransmitter release, where it is thought to increase priming of synaptic vesicles. Replacement of endogenous UNC-13 with a transgene expressing a non–DAG-binding *UNC-13* mutant [*UNC-13* (H173K), henceforth referred to as *UNC-13*(H173K) animals] causes aldicarb resistance, suggesting lowered levels of ACh release (Lackner *et al*., 1999; Nurrish *et al*., 1999; Richmond *et al*., 1999, 2001). In contrast,

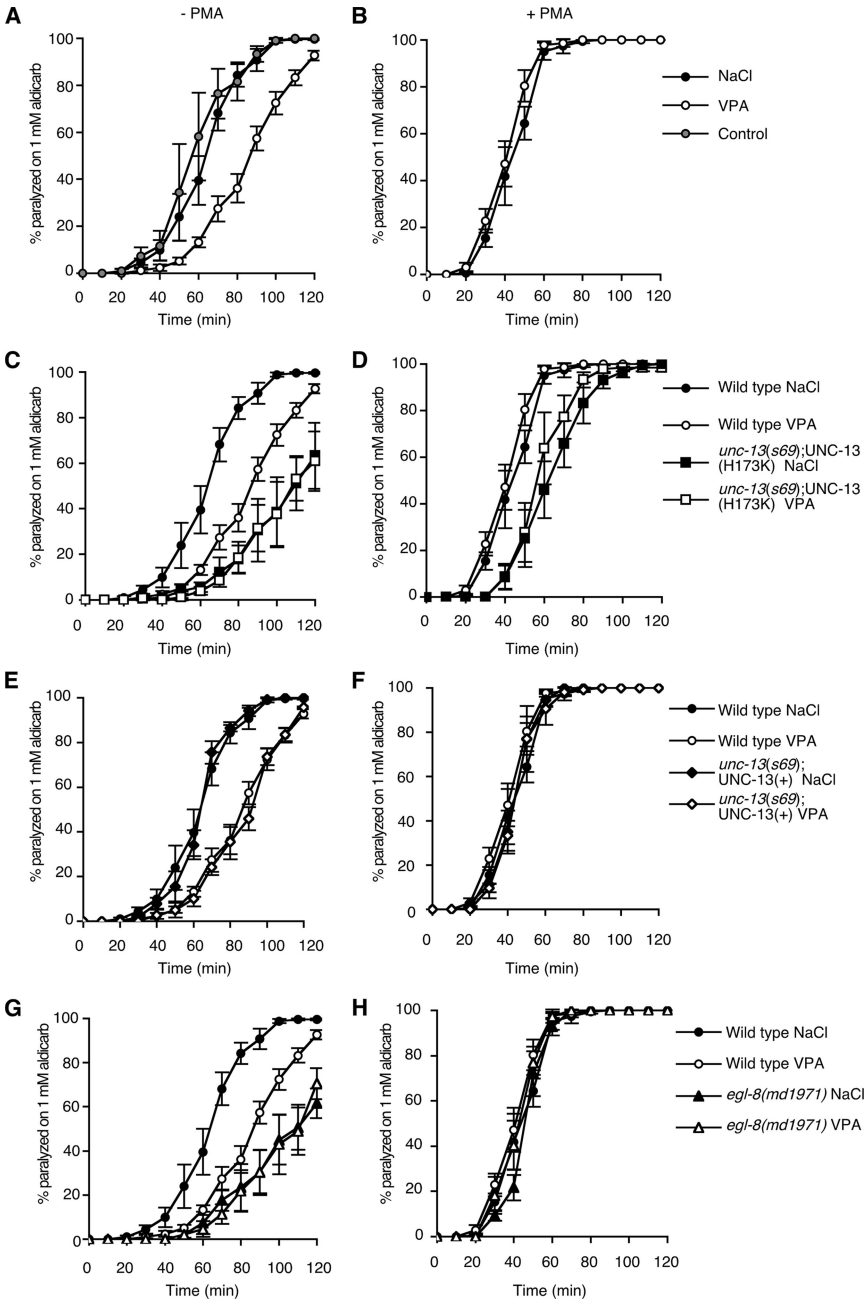

Figure 4. VPA reduces ACh release. Levels of ACh release were measured by determining rates of paralysis in the presence of the acetylcholinesterase inhibitor aldicarb either in the absence (A, C, E, and G) or presence of the phorbol ester PMA (B, D, F, and H). In all cases, there was no significant statistical difference between NaCl and VPA treatments when tested in the presence of PMA. (A and B) Exposure to 12 mM VPA caused animals to become resistant to aldicarb compared with untreated animals and animals exposed to 12 mM NaCl (A). Addition of the DAG analogue PMA caused hypersensitivity to aldicarb; this sensitivity was not altered by addition of 12 mM VPA or 12 mM NaCl (B). In A, at 80 min the percentage of animals paralyzed in the absence of drug was 81.6 ± 8.1%, on NaCl 84.2 ± 4.7%, on VPA 36.1 ± 6.0%; errors are SEM, using an unpaired Student's *t* test the difference between no drug and VPA, p = 0.0093, and between NaCl and VPA, p = 0.0002. There was no significant statistical difference for any of the drug treatments when combined with PMA. (C–F) *unc-13(s69)* animals were rescued with a transgene that expresses either a non–DAG-binding form of the UNC-13 neuromodulator [*unc-13(s69);UNC-13*(H173K)::GFP, referred to in the text as UNC-13(H173K) animals] (C and D) or by a transgene expressing a wild-type form of UNC-13 [*unc-13(s69);UNC-13*::GFP referred to in the text as UNC-13(+) animals] (E and F). UNC-13(H173K) animals are resistant to aldicarb (at 80 min, paralysis is 17.8 ± 6.0% SEM), and this is not further increased by the addition of 12 mM VPA (at 80 min, paralysis 18.5 ± 6.9% SEM, difference from NaCl, p = 0.9336 using unpaired Student's *t* test) (C). *unc-13(s69);UNC-13* (H173K) animals are partially resistant to the effects of PMA (D). VPA (12 mM) decreases the aldicarb sensitivity of UNC-13(+) animals the same as wild-type animals (at 80 min, on NaCl paralysis 86.3 ± 1.4% SEM compared with VPA paralysis 35.4 ± 7.7% SEM, p = 0.0003 using unpaired Student's *t* test) (E). UNC-13(+) animals are hypersensitive to aldicarb in the presence of PMA, and this sensitivity is not affected by exposure to 12 mM VPA (F). (G and H) A mutation in the EGL-8 PLBβ [*egl-8(md1971)*] results in resistance to aldicarb (at 80 min on NaCl paralysis is 23.5 ± 10.6% SEM), and this sensitivity is not further increased by the addition of 12 mM VPA (at 80 min, paralysis 21.8% ± 9.4, difference from NaCl, p = 0.9 using unpaired Student's *t* test) (G). Addition of the DAG analogue PMA caused hypersensitivity to aldicarb, this is not suppressed in *egl-8(md1971)* mutant animals (H).

unc-13(s69) mutant animals rescued by a transgene expressing a wild type UNC-13 [henceforth referred to as UNC-13(+) animals] have a wild-type response to aldicarb (Lackner *et al*., 1999; Sieburth *et al*., 2006). Addition of VPA to either *egl-8* PLCβ mutants or *UNC-13*(H173K) animals did not further decrease levels of ACh release (Figure 4, C and G), whereas UNC-13(+) animals responded to VPA the same as wild type (Figure 4E). Thus, both *egl-8* mutant animals and *UNC-13*(H173K) animals are resistant to the effects of VPA on ACh release. Interestingly, VPA still increases muscle sensitivity to levamisole in both *egl-8* mutant animals and *UNC-13*(H173K) animals (Supplemental Figure 2, B and C), suggesting that VPA effects on the muscle are independent of DAG signaling via EGL-8 and UNC-13 in neurons. Exposure to the DAG analogue PMA causes animals to paralyze much faster in the presence of aldicarb, suggesting a strong increase in levels of ACh release (Lackner *et al*., 1999; Miller *et al*., 1999). PMA caused wild-type, *egl-8* PLCβ mutants, and UNC-13(+) animals to be hypersensitive to the paralytic effects of aldicarb, and this sensitivity was not decreased by exposure to VPA (Figure 4, B, F, and H), whereas *UNC-13*(H173K) animals were only partially responsive to PMA (Figure 4D), as has been reported previously (Lackner *et al*., 1999; Sieburth *et al*., 2006). Thus, exposure to VPA more closely mimicked a defect in DAG

production than a defect in a DAG effector, suggesting that VPA decreases DAG production.

VPA Inhibits Recruitment of UNC-13 to Neurotransmitter Release Sites

We have previously shown that activation of muscarinic ACh signaling or inhibition of serotonin signaling increases ACh release in *C. elegans*. In both cases, increases in ACh release correlate with the enrichment of the DAG-binding UNC-13 neuromodulator to sites of neurotransmitter release sites (Lackner *et al*., 1999; Nurrish *et al*., 1999). The enrichment of UNC-13 at neurotransmitter release sites is due to increases of DAG. If VPA decreases DAG production, then it should reduce the accumulation of UNC-13 at neurotransmitter release sites. Addition of the serotonin antagonist methiothepin caused an *UNC-13*::YFP fusion protein to become punctate and increased sensitivity to aldicarb. Addition of VPA decreased both these effects; animals on VPA and methiothepin were less sensitive to aldicarb than animals on methiothepin alone, also VPA decreased the number of *UNC-13*::YFP puncta formed in response to addition of methiothepin (Figure 5, A and B). *UNC-13*::YFP acts as a marker of DAG accumulation as mutation of the DAG binding domain of UNC-13 [*UNC-13*(H173K)] prevented accumulation of UNC-13::YFP to sites of release upon decreases in serotonin signaling (Nurrish *et al*., 1999). We confirmed that VPA did not affect the number of release sites using a SNB-1::CFP fusion protein. Synaptobrevin (SNB)-1 is soluble *N*-ethylmaleimide-sensitive factor attachment protein receptor protein enriched in the synaptic vesicle membrane. The density of SNB-1::CFP puncta was unaltered by addition of VPA. The UNC-13::YFP puncta colocalized with SNB-1::CFP, demonstrating that UNC-13::YFP is recruited to sites of neurotransmitter release (Nurrish *et al*., 1999). These results are consistent with a model in which VPA decreases levels of DAG, leading to less UNC-13 present at neurotransmitter release sites.

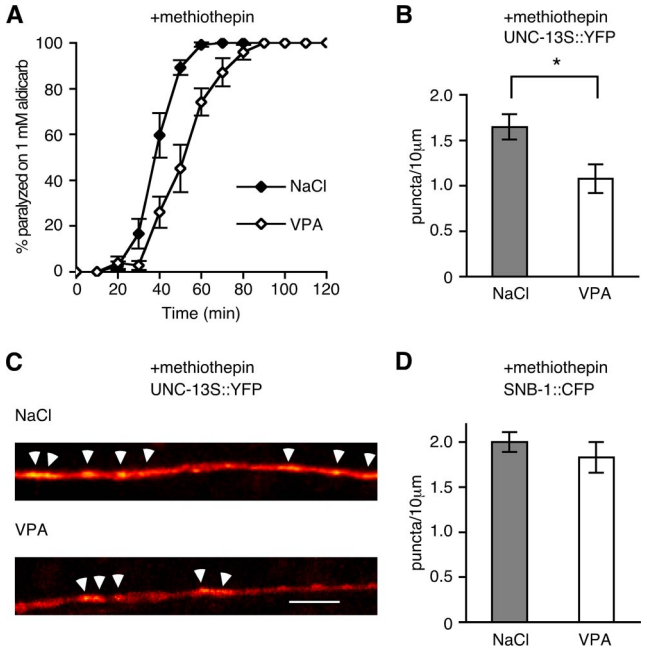

Figure 5. VPA decreases UNC-13 accumulation but not synapse numbers. (A) The serotonin antagonist methiothepin causes animals to become hypersensitive to aldicarb-induced paralysis. This effect is reversed by exposure to VPA (on methiothepin and NaCl paralysis at 60 min is 99.2% ± 0.9 SEM, on methiothepin and VPA paralysis is 74.1 ± 5.9% SEM, $p = 0.003$, using unpaired Student's *t* test). (B and C) The serotonin antagonist methiothepin causes *UNC-13*::YFP to become punctate in a DAG-dependent manner (Nurrish *et al*., 1999), and this is suppressed by exposure to 12 mM VPA. In B, each data point represents mean ± SEM from 14 animals ($p < 0.05$, Student's *t* test). In C, digital images were converted from grayscale into a 32-color lookup table (ImageJ) to visualize pixel intensities. Arrows point to puncta counted in B. Bar, 10 μm. (D) The integral membrane protein SNB-1::CFP is enriched in synaptic vesicles; thus, it acts as a marker for synaptic vesicle release sites. VPA did not alter the density of SNB-1::CFP puncta.

VPA Inhibits Egg-laying Behavior via DAG Signaling

To further assess the VPA effect on DAG-related signaling, we next examined egg-laying behavior, which is modulated by DAG production and DAG signaling. A 2-h exposure to VPA did not cause a significant decrease in total number of eggs due to ovulation defects; however, exposure to VPA caused wild-type and UNC-13(+) animals to lay fewer eggs, although UNC-13(+) animals laid fewer eggs than wild-type in the presence or absence of VPA (Figure 6, A and C). Defects in DAG production (PLCβ EGL-8) and DAG signaling [*UNC-13*(H173K) animals] caused fewer eggs to be laid, and this was not further reduced by exposure to VPA (Figure 6, B and D). Thus, VPA mimicked the decreased egg laying caused by defects in both DAG production and DAG signaling. That VPA could not further decrease egg laying in *egl-8* mutants or *UNC-13*(H173K) animals is consistent with a model in which VPA inhibition of egg laying requires both normal levels of DAG production and DAG signaling via UNC-13. In wild-type animals, VPA had no effect on egg laying in the presence of the DAG analogue PMA—the number of eggs laid by animals exposed to a combination of both VPA and PMA was similar to that of animals exposed to PMA alone (Figure 6E). Addition of PMA did not bypass the reduced egg laying caused by a defect in *UNC-13*(H173K) animals (Figure 6F). However, PMA did rescue the reduced egg laying caused by a defect in DAG production (*egl-8* mutants) both in the presence or absence of VPA (Figure 6G). Thus, our data support a model in which VPA reduces egg laying by decreases in DAG production but not signaling downstream of DAG.

pkc-1 Mutants Are Not Resistant to VPA

Full stimulation of ACh release by the DAG analogue PMA requires both UNC-13 and the DAG-activated protein kinase PKC-1 (Lackner *et al*., 1999; Sieburth *et al*., 2006). Mutations in *pkc-1* cause resistance to aldicarb due to defects in neuropeptide secretion from cholinergic motor neurons (Sieburth *et al*., 2006; Figure 7A). Thus, both PKC-1 and UNC-13 are required in cholinergic motor neurons for normal rates of paralysis on aldicarb. Mutations in both *unc-13* and *pkc-1* are required for complete suppression of the aldicarb hypersensitivity of animals exposed to PMA (Sieburth *et al*., 2006). However, in contrast to *unc-13* mutations, *pkc-1* mutant animals further increase their resistance to aldicarb when exposed to VPA (Figure 7A). *pkc-1* mutant animals laid fewer eggs than wild-type (Figure 7B), and VPA further decreased the number of eggs laid (Figure 7B). Thus, VPA can decrease two DAG-regulated behaviors, ACh release and egg laying, to a similar extent in both wild-type and *pkc-1* mutant animals, suggesting that VPA acts to inhibit DAG signaling via UNC-13 more strongly than DAG signaling through PKC-1.

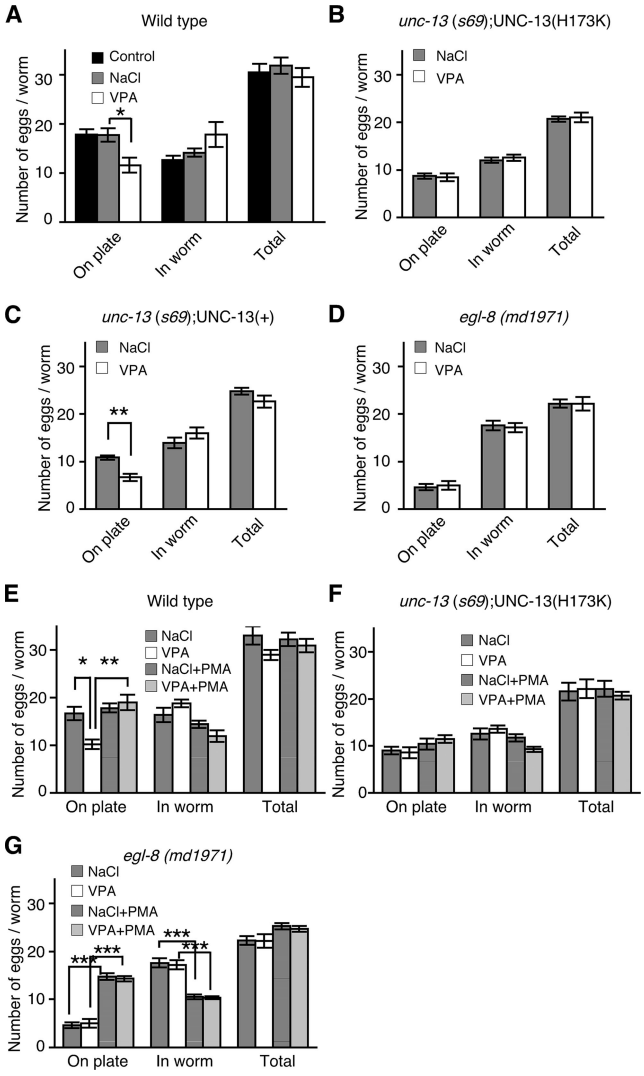

Figure 6. VPA inhibits egg-laying behavior via DAG signaling. The number of eggs laid on the plate over 2 h, and the number of eggs remaining in the animals at the end of the 2 h were determined. (A) VPA inhibits egg laying. Exposure to 6 mM VPA reduced the number of eggs laid on the plate compared with 6 mM NaCl (*$p < 0.05$, Student's *t* test). (B and C) *unc-13(s69)* animals were rescued with a transgene that expresses either a non–DAG-binding form of the UNC-13 neuromodulator [*unc-13(s69);UNC-13*(H173K)::GFP, referred to in the text as UNC-13(H173K) animals] (B) or by a transgene expressing a wild-type form of UNC-13 [*unc-13(s69);UNC-13*::GFP referred to in the text as UNC-13(+) animals] (C). Egg laying by UNC-13(H173K) animals is unaffected by addition of 6 mM VPA (B), whereas egg laying by UNC-13(+) animals is inhibited by 6 mM VPA (C). (D) A mutation in the EGL-8 PLBβ [*egl-8(md1971)*] causes an egg-laying defect, and this is not altered by addition of 6 mM VPA. (E–G) The addition of DAG analogue PMA reverses the inhibition of egg laying caused both by exposure to 6 mM VPA in wild-type (E) animals and by mutation of the PLCβ EGL-8 (G), but not the inhibition caused by disruption of a DAG effector, UNC-13(H173K) animals (F). Each datum represents mean ± SEM from five independent experiments. *$p < 0.05$, **$p < 0.01$, and ***$p < 0.001$, Scheffé's multiple comparison test.

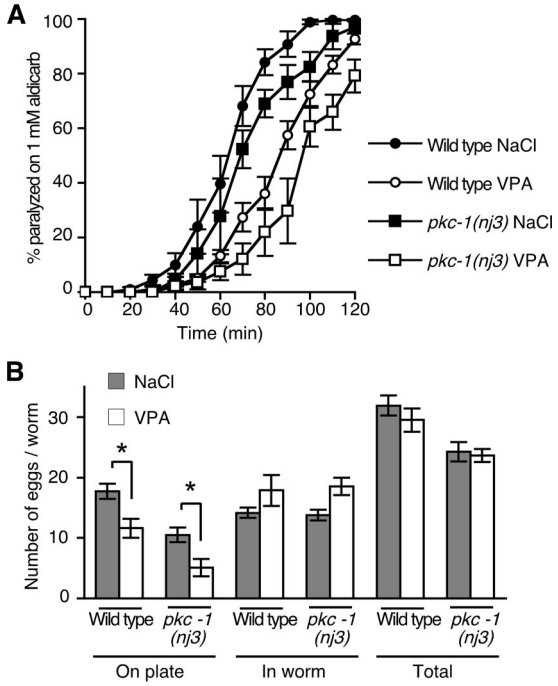

Figure 7. VPA inhibits ACh release and egg laying in a *pkc-1* mutant. (A) Levels of ACh release were measured by determining rates of paralysis in the presence of the acetylcholinesterase inhibitor aldicarb. *pkc-1(nj3)* mutant animals are resistant to aldicarb induced paralysis compared with wild type in the absence of salt (data not shown) and in the presence of 12 mM NaCl. Exposure to 12 mM VPA caused both wild-type and *pkc-1(nj3)* mutant animals to become resistant to aldicarb (For *pkc-1(nj3)*, paralysis at 80 min on NaCl is 68.9 ± 5.0% SEM, on VPA 21.9 ± 8.7% SEM, $p = 0.0008$, using unpaired Student's *t* test). (B) Exposure to 6 mM VPA caused *pkc-1(nj3)* mutant animals to lay fewer eggs on the plate than animals exposed to 6 mM NaCl. Exposure to 6 mM VPA did not affect the total number of eggs produced (*$p < 0.05$, Student's *t* test).

VPA Alters Inositol Phosphate Levels

Phospholipases generate IP_3 from PIP_2. A small proportion of IP_3 can be further phosphorylated to generate other inositol phosphates, such as IP_6. However, the majority of IP_3 enters the inositol cycle, and it is sequentially dephosphorylated to form inositol bisphosphate (IP_2), IP_1, and, ultimately, inositol, which can be used to produce phosphatidyl inositol (PI) (Figure 8A).

To test whether VPA alters the inositol polyphosphate profile, we fed tritiated inositol to living animals for 4 d, extracted the soluble inositol polyphosphates from whole animals, and studied the different species using HPLC. The inositol polyphosphate elution profile of untreated *C. elegans* was similar to that of *Saccharomyces cerevisiae* and mammalian cells, with an easily detectable IP_6 peak; the ratio of IP_6 to IP_1 or IP_2, however, was much smaller in *C. elegans* (Figure 8B). Addition of VPA caused a reduction in levels of IP_1 relative to IP_1 levels in control animals (Figure 8C), indicating that VPA alters inositol phosphate metabolism. However, we did not detect a significant change in levels of IP_2, IP_3, or IP_6 compared with controls, possibly for technical reasons (see *Discussion*).

VPA Does Not Decrease PIP_2 Levels

VPA causes behavioral defects consistent with decreases in both DAG and IP_3 levels. The simplest explanation for these results is that VPA inhibits either one or more PLCs or an enzyme required for PIP_2 production. In the former case, we would predict PIP_2 levels to be unchanged or increased, whereas in the latter case we would predict a decrease in

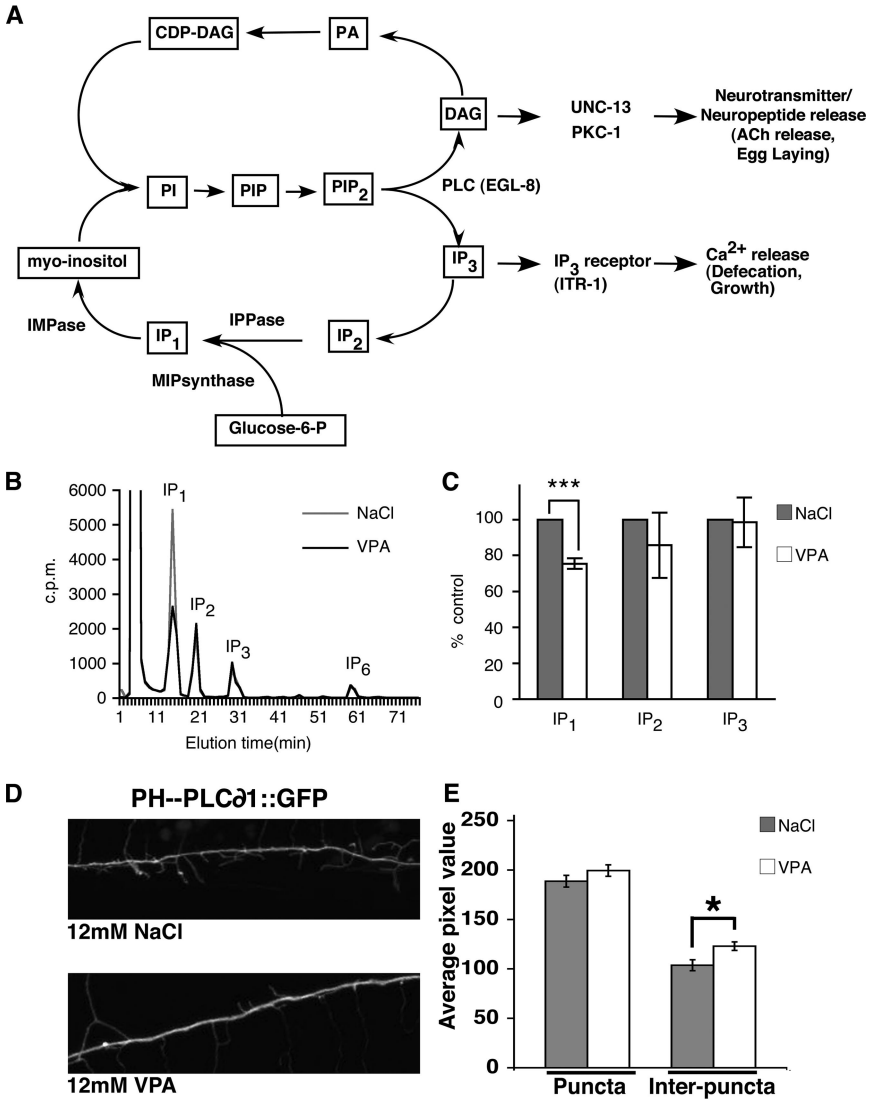

Figure 8. VPA decreases IP_1 and increases PIP_2. (A) Illustration of a simplified inositol phosphate cycle. $PI(4,5)P_2$ is hydrolyzed by PLC enzymes to generate IP_3 and DAG. IP_3 is degraded by sequential dephosphorylations to myoinositol. The enzymes IPPase and IMPase are sensitive to inhibition by lithium. MIP synthase catalyzes the conversion of glucose-6-phosphate (glucose-6-P) to IP_1 in inositol de novo synthesis. DAG is converted to phosphatidic acid (PA). PA is converted to cytidine diphosphodiacylglycerol (CDP-DAG). PI is synthesized from CDP-DAG and myoinositol by PI synthase. In *C. elegans* $Ins(1,4,5)P_3$ induces intracellular Ca^{2+} release, which is required for correct rates of defecation and growth. DAG acts via UNC-13 and PKC-1 to increase ACh release at neuromuscular junctions and stimulate egg laying. (B) Typical HPLC elution profiles of soluble inositol polyphosphates from *C. elegans* radiolabeled with [^{3}H]inositol for 4 d. Shown are elution profiles for animals exposed to 12 mM NaCl or VPA. IP_1, IP_2, IP_3, and IP_6. (C) VPA (12 mM) reduces levels of IP_1. Shown are the amounts of IP_1, IP_2, and IP_3 in animals treated with 12 mM VPA compared with animals treated with 12 mM NaCl (set to 100%). Levels of IP_2, IP_3, and IP_6 were not significantly changed. (D) The $PI(4,5)P_2$ reporter PHPLC-∂1::GFP expressed from the *rab-3* promoter has a punctate pattern in the sublateral dorsal nerve cord of wild-type animals exposed to either 12 mM NaCl (top) or 12 mM VPA (bottom). (E) Quantification of PHPLC-∂1::GFP fluorescence in the sublateral dorsal nerve cord. Average pixel intensity within puncta was unchanged by exposure to 12 mM VPA, although average pixel intensity between puncta was increased (***$p < 0.001$ and *$p < 0.01$, Student's *t* test; error bar, SEM).

PIP_2 levels. We first attempted to quantify PIP_2 levels as we had for inositol polyphosphates, but our results were too variable to give meaningful results. We therefore visualized PIP_2 levels using PHPLC-∂1::GFP, which binds selectively to $PtdIns(4,5)P_2$ (Varnai and Balla, 1998; Patton *et al*., 2005). We obtained animals expressing PHPLC-∂1::GFP from the pan-neuronal *rab-3* promoter that has been used in *C. elegans* to demonstrate changes in levels of PIP_2 in animals defective for polyunsaturated fatty acid production (Marza *et al*., 2007). As reported previously (Marza *et al*., 2007), we observed a punctate distribution of PHPLC-∂1::GFP in the sublateral neuronal processes of untreated animals (Figure 8D). We were unable to distinguish individual puncta in the dorsal and ventral cords because they contained too many neurons; therefore, we measured PHPLC-∂1::GFP fluorescence at sublateral neurons (Marza *et al*., 2007). On addition of 12 mM VPA, we observed a slight increase in the PHPLC-∂1::GFP fluorescence at puncta, but this was not statistically significant (189 ± 20 12 mM NaCl vs. 199 ± 20 12 mM VPA; $p = 0.2$) (Figure 8, D and E). VPA (12 mM) did cause a significant increase in the amount of PHPLC-∂1::GFP fluorescence present between puncta (103 ± 6 12 mM NaCl vs. 123 ± 15 12 mM VPA; $p = 0.01$) (Figure 8, D and E). Ideally, we would want to observe changes in PHPLC-∂1::GFP fluorescence in mutants predicted to have changes in PIP_2 levels. A mutation in the single *C. elegans ppk-1* would be expected to eliminate PIP_2; however, *ppk-1* mutations are lethal (Weinkove *et al*., 2008). Thus, the results with PHPLC-∂1::GFP must be treated with care, but they suggest that VPA does not decrease levels of PIP_2 within neurons, and they may act to slightly increase PIP_2 levels.

DISCUSSION

In this report, we show that VPA affects IP_3-regulated behaviors, defecation, and ovulation, confirming that VPA affects inositol signaling. We also show that VPA affects DAG-regulated behaviors locomotion and egg laying. VPA seems to affect DAG signaling via UNC-13 more than DAG signaling by PKC-1.

To test for a role of VPA in inositol phosphate signaling in *C. elegans*, we compared the effects of VPA with defects at three steps in this signaling pathway: a defect in production of inositol (RNAi knockdown of MIP synthase), inhibition of the inositol phosphate recycling enzymes IMPase and IPPase (addition of Li^+), and a defect in the IP_3 receptor (Dal

Santo *et al*., 1999; Walker *et al*., 2002). Exposure to VPA causes the same phenotype as all three of these methods of disrupting inositol phosphate signaling—increased defecation cycle length. In addition, VPA decreased ovulation, which is another IP_3-regulated behavior (Clandinin *et al*., 1998). An important question is whether VPA acts on IP_3 signaling directly or on a parallel signaling pathway. Gain-of-function mutations in the IP_3 Receptor have been shown to suppress defecation and ovulation defects caused by lowered amounts of IP_3 production (Yin *et al*., 2004; Espelt *et al*., 2005). The same IP_3 receptor gain-of-function mutations also suppress defects in ovulation and defecation caused by VPA. This suggests that VPA reduces levels of IP_3 signaling at a point upstream of the IP_3 receptor, probably by inhibiting IP_3 production. VPA has also been shown to decrease inositol phosphate signaling, in particular IP_3 signaling, in mammalian neuronal cell cultures and in *Dictyostelium* (Williams *et al*., 2002). Extraction of labeled inositol phosphates from whole *C. elegans* revealed that VPA does decrease IP_1, although levels of IP_3 are not significantly affected. This conflicts with behavioral assays that predict a defect in IP_3 levels. Our chromatographic analyses do not allow the separation of the different isomeric inositol polyphosphates species; the IP_3 peak is therefore a mixture of the several IP_3 isomers, and we cannot conclude that levels of I(1,4,5)P_3 are unchanged. In addition, the target of VPA may only exist in a subset of cells, and so changes in IP_3 levels in a small number of cells may not be detected when assaying whole animals. It is also possible that IP_1 itself may have an important role in the control of both defecation and ovulation and that VPA alters both by decreasing IP_1 levels, although IP_3 receptor gain-of-function mutations suppressed VPA-mediated defects in both defecation and ovulation, suggesting that VPA does alter both behaviors by changing IP_3 levels. Improvements in the detection of labeled inositol phosphates would allow us to tell which is the correct explanation. Nontheless, PLC-generated I(1,4,5)P_3 is rapidly metabolized and recycled through the "inositol cycle" (Figure 7A) to form inositol. IP_1 is a key element of this important metabolic cycle, and its significant decrease after exposure to VPA suggests that VPA alters both inositol phosphate recycling and signaling.

RNAi of MIP synthase should decrease the formation of inositol from glucose, an effect that should be relieved by addition of inositol. Indeed, addition of 200 mM myoinositol rescues the thermotaxis defects in *ttx-7* (IMPase) mutants, which cannot produce inositol (Tanizawa *et al*., 2006). However, 200 mM myoinositol caused defecation defects to wild-type animals (data not shown), and we were unable to test whether myoinositol could rescue the defects caused by exposure to VPA.

In addition to the inhibition of IP_3-regulated behaviors by VPA, we show that VPA inhibits DAG-regulated behaviors—ACh release and egg laying. In the first case, exposure to VPA decreases levels of ACh released by motor neurons onto body wall muscles, as shown by a decreased rate of paralysis by aldicarb. In the second case, VPA decreases the rate of egg laying. In both cases, VPA mimics mutations in *egl-8* PLCβ, *pkc-1*, and animals in which a severe *unc-13* mutant is rescued by a transgene expressing a non–DAG-binding UNC-13 mutant (*UNC-13*(H173K) animals). Addition of VPA does not further decrease locomotion and egg laying in either *egl-8* PLCβ mutants or *UNC-13*(H173K) animals. However, in *pkc-1* mutants, VPA is still able to reduce both ACh release (as shown by increased resistance to aldicarb) and egg laying. We cannot definitely rule out an effect of VPA on signaling via PKC-1, but it does seem that DAG signaling via UNC-13 is more sensitive to VPA than DAG signaling via PKC-1. It is also possible that VPA affects DAG signaling via other DAG effectors, for example, other PKCs.

What is the relevant target(s) of VPA? In mammals, VPA has been shown to inhibit the activity of a prolyl oligopeptidase (Cheng *et al*., 2005); however, there is no obvious orthologue in *C. elegans*. Thus, the relevant VPA target(s) remains to be identified in *C. elegans*. Our data show that VPA acts to inhibit behaviors regulated by both inositol phosphates and DAG. Because both DAG and IP_3 are derived from PIP_2, it is possible that VPA causes a defect at or before PIP_2 production (Figure 7A). Use of a PIP_2 reporter suggests than neuronal levels of PIP_2 are slightly increased upon exposure to VPA. The simplest explanation for these data are that VPA inhibits a step after the production of PIP_2 but before the production of DAG and IP_3, probably all or a subset of PLCs, or a common regulator of PLCs. Alternatively, VPA could inhibit the removal of PIP_2 by a lipid phosphatase such as synaptojanin (UNC-26) (Harris *et al*., 2000), causing an increase in PIP_2 levels. We observed that PIP_2 levels were higher between the normal sites of PIP_2 accumulation, and this could cause a delocalization of PIP_2 binding effectors, leading to a decrease in the ability to generate DAG and inositol phosphates. VPA also caused an increase in muscle response to the nicotinic agonist levamisole, and this occurred independently of signaling via EGL-8 and UNC-13. Currently, we do not know whether VPA alters muscle responsiveness via changes in DAG and/or IP_3 signaling, or via a third mechanism.

VPA inhibited both defecation and ACh release in adults within 2 h, suggesting VPA acts to disrupt neuronal function and not development. The concentration of VPA (6–12 mM) used is ~10-fold higher than the recommended therapeutic blood serum concentrations (0.3–0.6 mM); however, we can only measure the external VPA concentration. Because of the relatively impermeable *C. elegans* cuticle it is likely the actual internal VPA concentration will be much closer to those used to treat bipolar disorder in humans. Thus, signaling pathways disrupted in *C. elegans* may be the same pathways disrupted in humans treated with VPA. Our results raise the possibility that VPA relieves the symptoms of bipolar disorder due to its action on DAG signaling pathways that regulate neurotransmitter release. However, both DAG and inositol phosphates have been implicated in the regulation of neuronal function, and we favor a model in which VPA helps control the symptoms of bipolar disorder by regulating neuronal function through its effects on both inositol phosphate and DAG signaling pathways.

ACKNOWLEDGMENTS

We thank other members of the Nurrish laboratory for advice and discussion, and Anne Mudge, Martin Raff, and Giovanni Lesa for comments on the manuscript. Strains were obtained from the *C. elegans* Genetics Center, which is supported by the National Institute of Health National Center for Research Resources. S.M.T. was supported by the Ernst Schering Foundation.

REFERENCES

Acharya, J. K., Labarca, P., Delgado, R., Jalink, K., and Zuker, C. S. (1998). Synaptic defects and compensatory regulation of inositol metabolism in inositol polyphosphate 1-phosphatase mutants. Neuron *20*, 1219–1229.

Allison, J. H., Boshans, R. L., Hallcher, L. M., Packman, P. M., and Sherman, W. R. (1980). The effects of lithium on myo-inositol levels in layers of frontal cerebral cortex, in cerebellum, and in corpus callosum of the rat. J. Neurochem. *34*, 456–458.

Azevedo, C., and Saiardi, A. (2006). Extraction and analysis of soluble inositol polyphosphates from yeast. Nat. Protoc. *1*, 2416–2422.

Betz, A., Ashery, U., Rickmann, M., Augustin, I., Neher, E., Sudhof, T. C., Rettig, J., and Brose, N. (1998). Munc13-1 is a presynaptic phorbol ester receptor that enhances neurotransmitter release. Neuron *21*, 123–136.

Brenner, S. (1974). The genetics of *Caenorhabditis elegans*. Genetics *77*, 71–94.

Cheng, L., Lumb, M., Polgar, L., and Mudge, A. W. (2005). How can the mood stabilizer VPA limit both mania and depression? Mol. Cell Neurosci. *29*, 155–161.

Clandinin, T. R., DeModena, J. A., and Sternberg, P. W. (1998). Inositol trisphosphate mediates a RAS-independent response to LET-23 receptor tyrosine kinase activation in *C. elegans*. Cell *92*, 523–533.

Dal Santo, P., Logan, M. A., Chisholm, A. D., and Jorgensen, E. M. (1999). The inositol trisphosphate receptor regulates a 50-second behavioral rhythm in *C. elegans*. Cell *98*, 757–767.

De Camilli, P., Emr, S. D., McPherson, P. S., and Novick, P. (1996). Phosphoinositides as regulators in membrane traffic. Science *271*, 1533–1539.

Espelt, M. V., Estevez, A. Y., Yin, X., and Strange, K. (2005). Oscillatory Ca2+ signaling in the isolated *Caenorhabditis elegans* intestine: role of the inositol-1,4,5-trisphosphate receptor and phospholipases C beta and gamma. J. Gen. Physiol. *126*, 379–392.

Fukuda, M., and Mikoshiba, K. (1997). The function of inositol high polyphosphate binding proteins. Bioessays *19*, 593–603.

Hallcher, L. M., and Sherman, W. R. (1980). The effects of lithium ion and other agents on the activity of myo-inositol-1-phosphatase from bovine brain. J. Biol. Chem. *255*, 10896–10901.

Harris, T. W., Hartwieg, E., Horvitz, H. R., and Jorgensen, E. M. (2000). Mutations in synaptojanin disrupt synaptic vesicle recycling. J. Cell Biol. *150*, 589–600.

Harwood, A. J. (2005). Lithium and bipolar mood disorder: the inositol-depletion hypothesis revisited. Mol. Psychiatry *10*, 117–126.

Horwood, J. M., Dufour, F., Laroche, S., and Davis, S. (2006). Signalling mechanisms mediated by the phosphoinositide 3-kinase/Akt cascade in synaptic plasticity and memory in the rat. Eur. J. Neurosci. *23*, 3375–3384.

Inhorn, R. C., and Majerus, P. W. (1987). Inositol polyphosphate 1-phosphatase from calf brain. Purification and inhibition by Li+, Ca2+, and Mn2+. J. Biol. Chem. *262*, 15946–15952.

Kamath, R. S. *et al*. (2003). Systematic functional analysis of the *Caenorhabditis elegans* genome using RNAi. Nature *421*, 231–237.

Karpova, A., Sanna, P. P., and Behnisch, T. (2006). Involvement of multiple phosphatidylinositol 3-kinase-dependent pathways in the persistence of late-phase long term potentiation expression. Neuroscience *137*, 833–841.

Lackner, M. R., Nurrish, S. J., and Kaplan, J. M. (1999). Facilitation of synaptic transmission by EGL-30 Gqalpha and EGL-8 PLCbeta: DAG binding to UNC-13 is required to stimulate acetylcholine release. Neuron *24*, 335–346.

Loscher, W. (1999). Valproate: a reappraisal of its pharmacodynamic properties and mechanisms of action. Prog. Neurobiol. *58*, 31–59.

Marza, E., Long, T., Saiardi, A., Sumakovic, M., Eimer, S., Hall, D. H., and Lesa, G. M. (2008). Polyunsaturated fatty acids influence synaptojanin localization to regulate synaptic vesicle recycling. Mol. Biol. Cell *19*, 833–842.

McCarter, J., Bartlett, B., Dang, T., and Schedl, T. (1999). On the control of oocyte meiotic maturation and ovulation in *Caenorhabditis elegans*. Dev. Biol. *205*, 111–128.

McMullan, R., Hiley, E., Morrison, P., and Nurrish, S. J. (2006). Rho is a presynaptic activator of neurotransmitter release at pre-existing synapses in *C. elegans*. Genes Dev. *20*, 65–76.

McMullan, R., and Nurrish, S. J. (2007). Rho deep in thought. Genes Dev. *21*, 2677–2682.

McPherson, P. S., Garcia, E. P., Slepnev, V. I., David, C., Zhang, X., Grabs, D., Sossin, W. S., Bauerfeind, R., Nemoto, Y., and De Camilli, P. (1996). A presynaptic inositol-5-phosphatase. Nature *379*, 353–357.

Miller, K. G., Alfonso, A., Nguyen, M., Crowell, J. A., Johnson, C. D., and Rand, J. B. (1996). A genetic selection for *Caenorhabditis elegans* synaptic transmission mutants. Proc. Natl. Acad. Sci. USA. *93*, 12593–12598.

Miller, K. G., Emerson, M. D., and Rand, J. B. (1999). Goalpha and diacylglycerol kinase negatively regulate the Gqalpha pathway in *C. elegans*. Neuron *24*, 323–333.

Miller, M. A., Ruest, P. J., Kosinski, M., Hanks, S. K., and Greenstein, D. (2003). An Eph receptor sperm-sensing control mechanism for oocyte meiotic maturation in *Caenorhabditis elegans*. Genes Dev. *17*, 187–200.

Nguyen, M., Alfonso, A., Johnson, C. D., and Rand, J. B. (1995). *Caenorhabditis elegans* mutants resistant to inhibitors of acetylcholinesterase. Genetics *140*, 527–535.

Nonet, M. L., Grundahl, K., Meyer, B. J., and Rand, J. B. (1993). Synaptic function is impaired but not eliminated in *C. elegans* mutants lacking synaptotagmin. Cell *73*, 1291–1305.

Nurrish, S., Segalat, L., and Kaplan, J. M. (1999). Serotonin inhibition of synaptic transmission: Galpha(0) decreases the abundance of UNC-13 at release sites. Neuron *24*, 231–242.

O'Donnell, T., Rotzinger, S., Nakashima, T. T., Hanstock, C. C., Ulrich, M., and Silverstone, P. H. (2000). Chronic lithium and sodium valproate both decrease the concentration of myo-inositol and increase the concentration of inositol monophosphates in rat brain. Brain Res. *880*, 84–91.

Okochi, Y., Kimura, K. D., Ohta, A., and Mori, I. (2005). Diverse regulation of sensory signaling by *C. elegans* nPKC-epsilon/eta TTX-4. EMBO J. *24*, 2127–2137.

Patton, A., Knuth, S., Schaheen, B., Dang, H., Greenwald, I., and Fares, H. (2005). Endocytosis function of a ligand-gated ion channel homolog in *Caenorhabditis elegans*. Curr. Biol. *15*, 1045–1050.

Phiel, C. J., Zhang, F., Huang, E. Y., Guenther, M. G., Lazar, M. A., and Klein, P. S. (2001). Histone deacetylase is a direct target of valproic acid, a potent anticonvulsant, mood stabilizer, and teratogen. J. Biol. Chem. *276*, 36734–36741.

Raymond, C. R., Redman, S. J., and Crouch, M. F. (2002). The phosphoinositide 3-kinase and p70 S6 kinase regulate long-term potentiation in hippocampal neurons. Neuroscience *109*, 531–536.

Richmond, J. E., Davis, W. S., and Jorgensen, E. M. (1999). UNC-13 is required for synaptic vesicle fusion in *C. elegans*. Nat. Neurosci. *2*, 959–964.

Richmond, J. E., Weimer, R. M., and Jorgensen, E. M. (2001). An open form of syntaxin bypasses the requirement for UNC-13 in vesicle priming. Nature *412*, 338–341.

Shaltiel, G., Shamir, A., Shapiro, J., Ding, D., Dalton, E., Bialer, M., Harwood, A. J., Belmaker, R. H., Greenberg, M. L., and Agam, G. (2004). Valproate decreases inositol biosynthesis. Biol. Psychiatry *56*, 868–874.

Sieburth, D., Madison, J. M., and Kaplan, J. M. (2006). PKC-1 regulates secretion of neuropeptides. Nat. Neurosci. 10, 49–57.

Stiernagle, T. (2006). Maintenance of *C. elegans*. WormBook 1–11.

Tanizawa, Y., Kuhara, A., Inada, H., Kodama, E., Mizuno, T., and Mori, I. (2006). Inositol monophosphatase regulates localization of synaptic components and behavior in the mature nervous system of *C. elegans*. Genes Dev. *20*, 3296–3310.

Thomas, J. H. (1990). Genetic analysis of defecation in *Caenorhabditis elegans*. Genetics *124*, 855–872.

Varnai, P., and Balla, T. (1998). Visualization of phosphoinositides that bind pleckstrin homology domains: calcium- and agonist-induced dynamic changes and relationship to myo-[^{3}H]inositol-labeled phosphoinositide pools. J. Cell Biol. *143*, 501–510.

Walker, D. S., Gower, N. J., Ly, S., Bradley, G. L., and Baylis, H. A. (2002). Regulated disruption of inositol 1,4,5-trisphosphate signaling in *Caenorhabditis elegans* reveals new functions in feeding and embryogenesis. Mol. Biol. Cell *13*, 1329–1337.

Weinkove, D., Bastiani, M., Chessa, T. A., Joshi, D., Hauth, L., Cooke, F. T., Divecha, N., and Schuske, K. (2008). Overexpression of PPK-1, the *Caenorhabditis elegans* Type I PIP kinase, inhibits growth cone collapse in the developing nervous system and causes axonal degeneration in adults. Dev. Biol. *313*, 384–397.

Williams, R. S., Cheng, L., Mudge, A. W., and Harwood, A. J. (2002). A common mechanism of action for three mood-stabilizing drugs. Nature *417*, 292–295.

Xu, X., Guo, H., Wycuff, D. L., and Lee, M. (2007). Role of phosphatidylinositol-4-phosphate 5′ kinase (ppk-1) in ovulation of *Caenorhabditis elegans*. Exp. Cell Res. *313*, 2465–2475.

Yin, X., Gower, N. J., Baylis, H. A., and Strange, K. (2004). Inositol 1,4,5-trisphosphate signaling regulates rhythmic contractile activity of myoepithelial sheath cells in *Caenorhabditis elegans*. Mol. Biol. Cell *15*, 3938–3949.